REPORTS OF THE SWEDISH DEEP-SEA EXPEDITION. VOL. III
PHYSICS AND CHEMISTRY. NO. 6

THE EQUATORIAL CURRENTS IN THE PACIFIC OCEAN

BY

N. G. JERLOV

When the programme of the Swedish Deep-ea Expedition was drawn up, accurate oce-nographic data from the equatorial current ystem in the Pacific had been collected only rom the seventh cruise of the *Carnegie* during 928—29. It was found highly desirable to btain further information by crossing the quatorial current by some sections with serial bservations. In forming the working scheme ve had the great benefit of expert advice by . PALMÉN. The extensive observations had o be limited to the eastern and central part f the Pacific in order to fit them into the ighly limited time-table of the cruise. Here zig-zag course was laid out comprising four ections of which only the third was in a nearly neridional direction.

The *Albatross* left Panama on 28 August 947. Some stations (43—52) were occupied n the Gulf of Panama and in the vicinity of he Galapagos Islands. The first section, hich was started in the beginning of Septem-er, was oblique, nearly parallel to the Ameri-an coast, from the Galapagos Islands to 7° 46′ N (Fig. 1, Table 1). At this point the ourse was set for the Marquesas Islands and xtended across the Equator to 3°S where ne ship arrived on 9 October. The third sec-on, Tahiti-Hawaii, was run in November in a nearly meridional direction. The serial work along the fourth section, ending south of the Equator near long. 180 ° was finished before the end of the year. During the continued course westwards only 5 stations were occupied, the first one (Station 143) at the Equator, the others somewhat to the north.

The Pacific net included a total of 59 stations. Within the sections the spacing of stations was about 120 nautical miles and the time interval between them generally about 24 hours. The serial observations were usually limited to the uppermost 1,000 m but at nineteen selected stations — always at the Equator — extended to the proximity of the bottom. Between the stations, surface observations of temperature and salinity were made every hour, *i. e.* about every 7th mile, and bathythermograms for the depth range 0—130 m were taken every 4th hour (about every 30th mile). The methods employed are described in some detail in this volume, No. 4. The physical and chemical data are rendered in the appendix, Table 1; the interpolated values of temperature, salinity, and density as well as the computed anomalies of dynamic height at standard depths are tabulated in the appendix, Table 2.

This report will present data which contri-

TABLE 1. Oceanographic sections in the Pacific.

Section	Time	Station	Latitude	Longitude
1	September 8—28	55— 80	2° 44′ S—17° 46′ N	92° 45′ W—126° 51′ W
2	September 8—October 9	80— 94	17° 46′ N— 3° 00′ S	126° 51′ W—136° 26′ W
3	November 5—25	102—123	13° 25′ S—15° 14′ N	149° 30′ W—152° 49′ W
4	December 17—26.....	126—138	14° 39′ N— 2° 37′ S	164° 50′ W—177° 45′ W

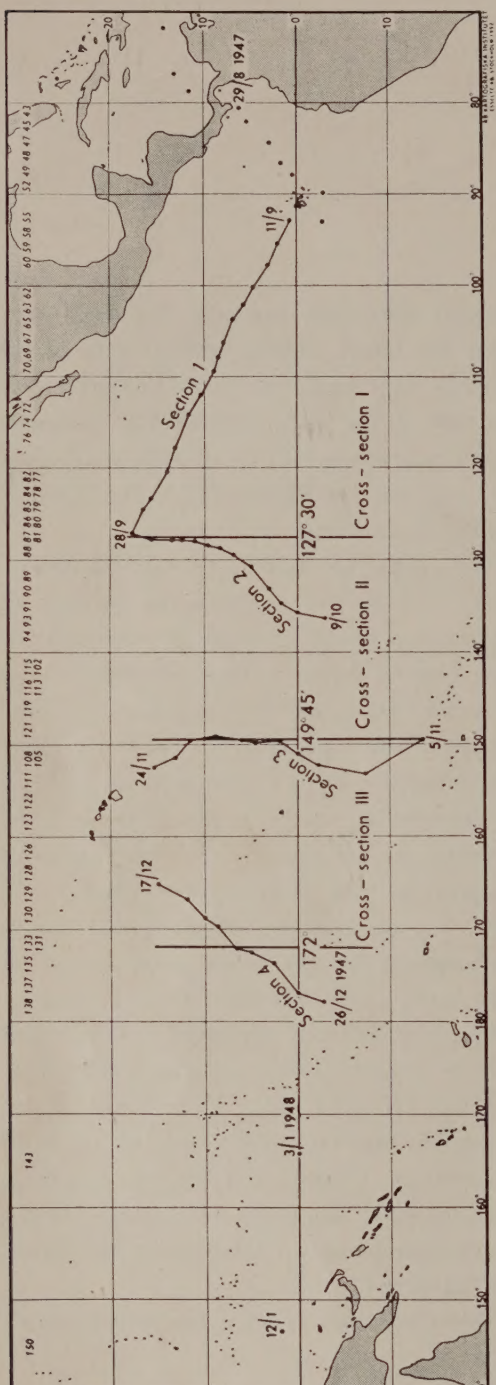

Fig. 1. Track chart for the *Albatross* cruise in the Pacific 28 August 1947—25 January 1948. Solid dots, hydrographic stations, 43—162.

bute to the knowledge of the flow of th equatorial currents in the autumn, and provid supplementary experimental information fo the understanding of the nature of the currents The theoretical interpretation of the equatoria water structure and water movements is nov in rapid progress. After the Swedish *Albatros* cruised in the Pacific, large-scale researc programmes for exploring the equatorial region have been set up by institutions in the U. S. A Several cruises have already been made an numerous data, mostly for the season January —March, have already been published in brie descriptive reports (CROMWELL, 1951, 1954 AUSTIN, 1954 a and b; STROUP, 1954). Othe experimental results are in the press (WOOSTER) These investigations give representations o water properties in vertical cross-sections Reference to them is made here only in excep tional cases in order to establish deviations o to stress some important point.

Thus, the discussion below has the presen data in view. Attention is chiefly focused o the physical features and the major current in the equatorial Pacific. The interpretatio of the chemical data is given in a separat chapter in this volume.

A preliminary report on the results gaine appeared earlier (JERLOV, 1953 b).

Horizontal Distribution of Properties

As the sections are not comparable i time the horizontal representation canno yield any clear synoptic picture. Nevertheles isopleths have been drawn between th sections in order to illustrate the horizonta distributions.

SVERDRUP (1944) has undertaken a systemati comparison of the *Carnegie* observations an the values from the SCHOTT charts and ha found that the deviations are not of a seriou character considering that the Schott chart represent only approximately the mean annua isopleths. In so far as the present distribution

ıow new features compared with the old con-
ɔpt these are discussed.

The pattern of surface salinity reflects the
estward transport of fairly high-salinity water
y the South Equatorial Current as well as the
ctension of low-salinity water from the coast
Central America which is associated with
ıe belt of high rainfall (Fig 2). The 34 ‰
ohaline has two branches in Sections 1—3 but
s trend between Section 2 and 3 is not fully
tablished.

Naturally the surface temperature is subject
great seasonal variations, due to heating and
ɔoling. Section 1 is characterized by a large
ea of 27° C water typical for the summer
tuation but the two 27° isotherms converge
ɔward Section 3 which represents November
ɔnditions (Fig. 3). In the general survey of
ıe surface temperature distribution the tongue
cold water from the Galapagos region to-
ards the west is as usual most conspicuous.
minimum temperature of 19°.2 is encounter-
l just south of these Islands.

The annual change of the temperature at
)0 m is little influenced by heating effects but
is apparently related to displacements of the
quatorial currents (SVERDRUP, 1944). The
otherms at 200 m in Fig. 4 are plotted with
ıe regard to the Schott chart in the western
ırt of the ocean. Values for Stations 89 and
35, which are too high, 20°.1 and 22°.8 respec-
vely, to fit into the general pattern, have
ɛen omitted. These localities are at the bound-
y between the South Equatorial Current
ıd the Countercurrent, both flowing with
eat velocity. This sharp edge, which is
idently of a transient nature, is asso-
ated with an unusually low discontinuity
yer.

The salient features in Fig. 4 are the two
ngues of low temperature one at the Equator
< 13°), the other north of it (< 11°). The
tter is present almost over the whole ocean
though only as a narrow strip in the eastern
ırt. On the whole, the temperature at 200 m
in the northern regions of Sections 1 and 2 is fairly high compared with the Schott and the *Carnegie* charts which show a tongue of cold water less than 10° extending from the Californian coast.

In the temperature distribution at 400 m the two belts of low temperature are recognized (Fig. 5). They are separated by a neck with temperature above 10° which is much narrower in its eastern part than that on the Schott chart. In the light of the new data it is evident that small seasonal fluctuations in temperature also occur at this level.

The distribution of the density brings out the major features in the current system (Fig. 6). In particular it is noticed that the water of minimum density, $\sigma_t < 21.5$, is present far towards the west.

Finally it is aimed to secure a significant horizontal representation of the amount of suspended matter as determined by Tyndall measurements (this volume, No. 3). The average particle content from the surface down to 50 m was chosen as being most representative. This water column comprises the chief part of the *euphotic* zone in the oceans and is still above the discontinuity layer for all stations except those in the Gulf of Panama.

The Tyndall values reflect the amount of plankton, mainly phytoplankton, and of *detritus* and are thus closely related to the organic production in the ocean. Surface strata, where an enrichment with nutrients takes place due to upwelling in a strict sense or to mixing between deep water and surface water, are usually rich in plankton. Regions with sinking water, especially in convergence regions, are poor. The pattern depicted in Fig. 7 reveals the striking difference between the eastern and the western areas of the equatorial region, the former being also fed by the highly fertile water from the upwelling region near the South American coast. The maximum belt near 10° N is attributed to dynamical features. On the route of the *Albatross* a minimum of

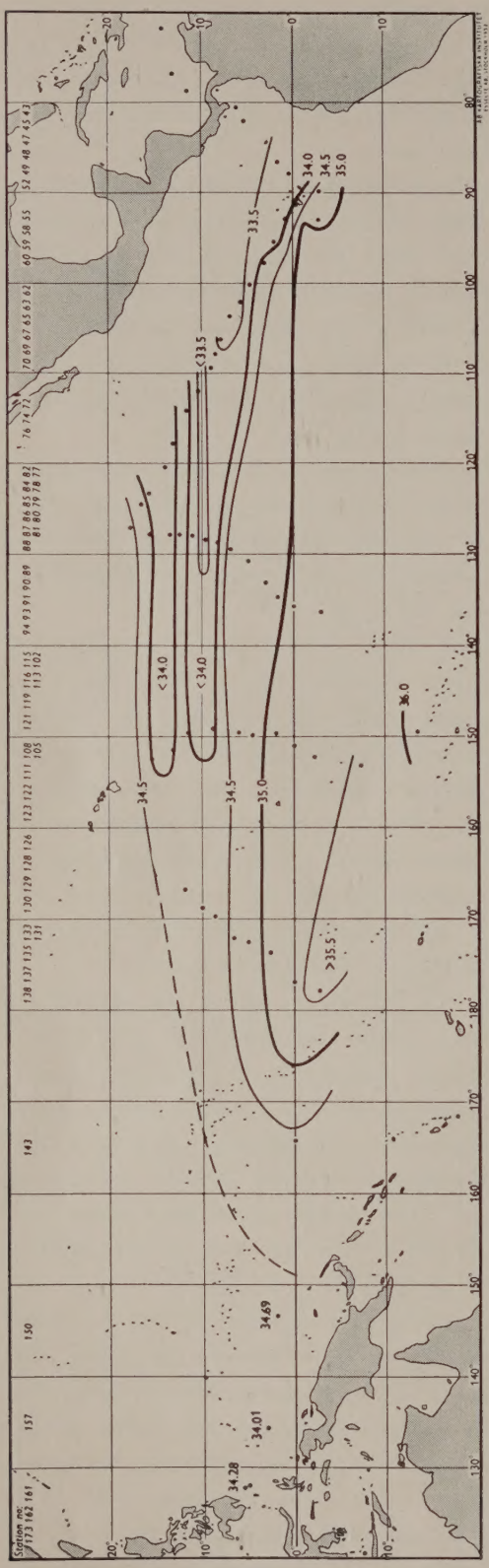

Fig. 2. Horizontal distribution of salinity at surface.

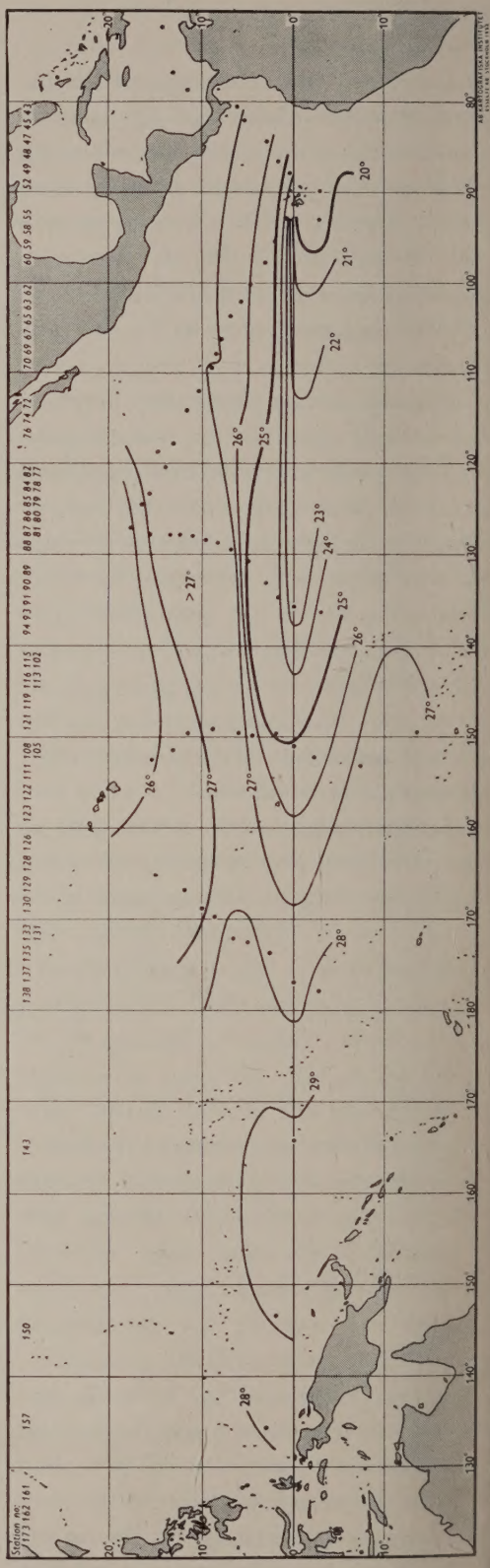

Fig. 3. Horizontal distribution of temperature at surface.

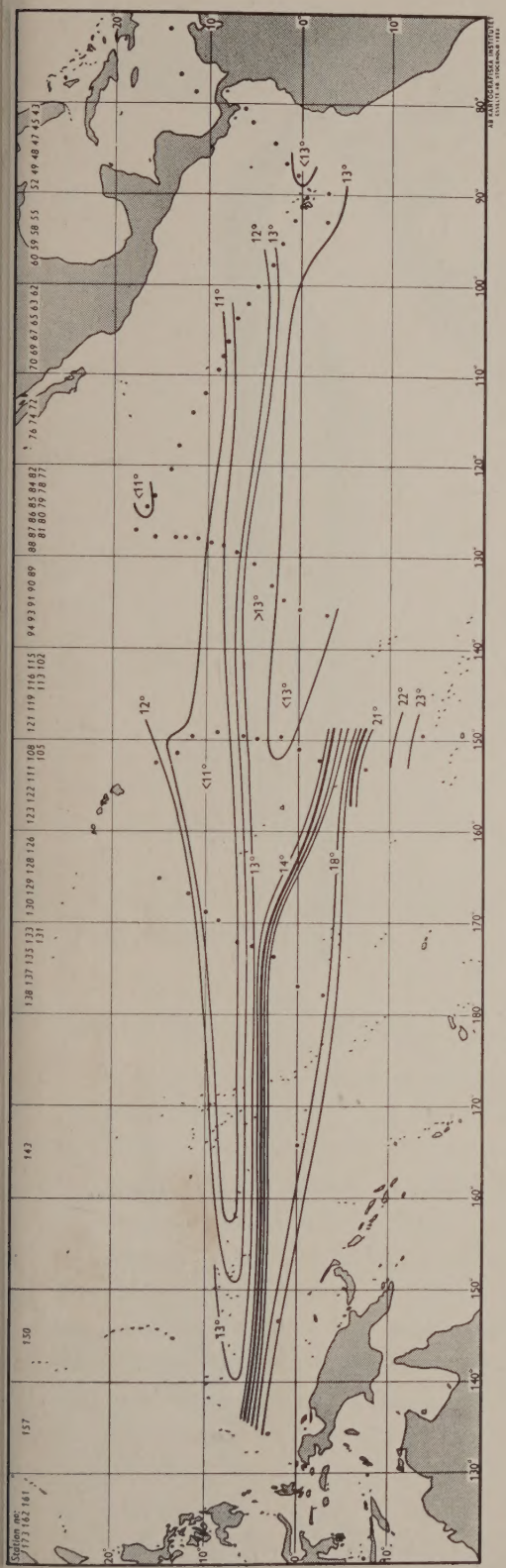

Fig. 4. Horizontal distribution of temperature at 200 m.

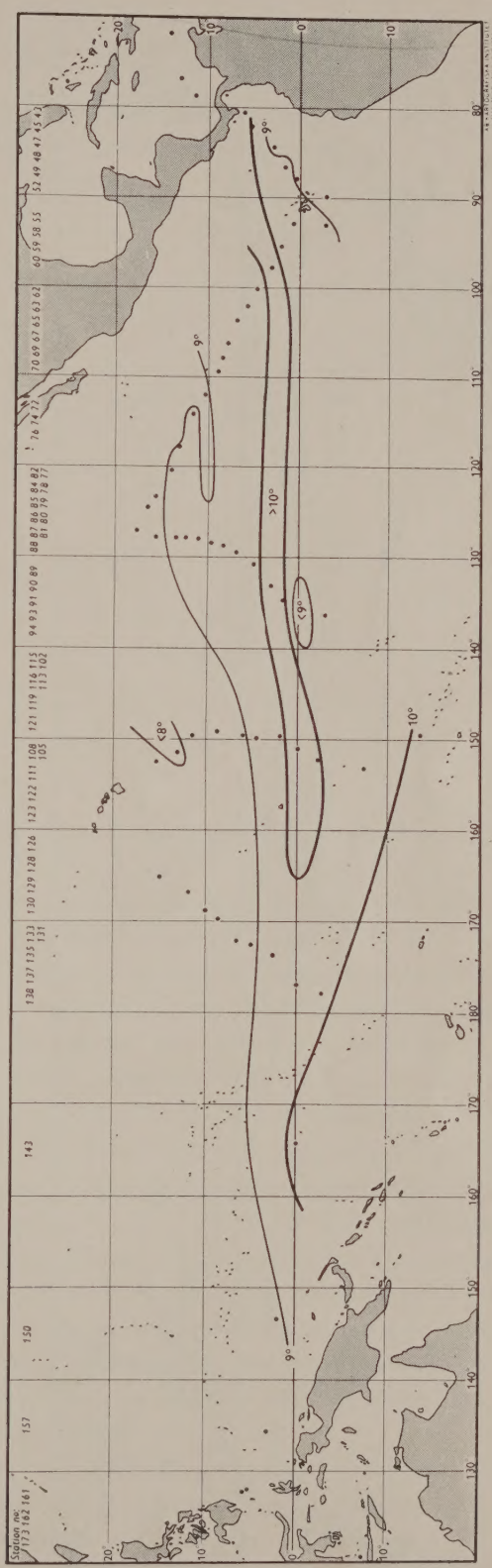

Fig. 5. Horizontal distribution of temperature at 400 m.

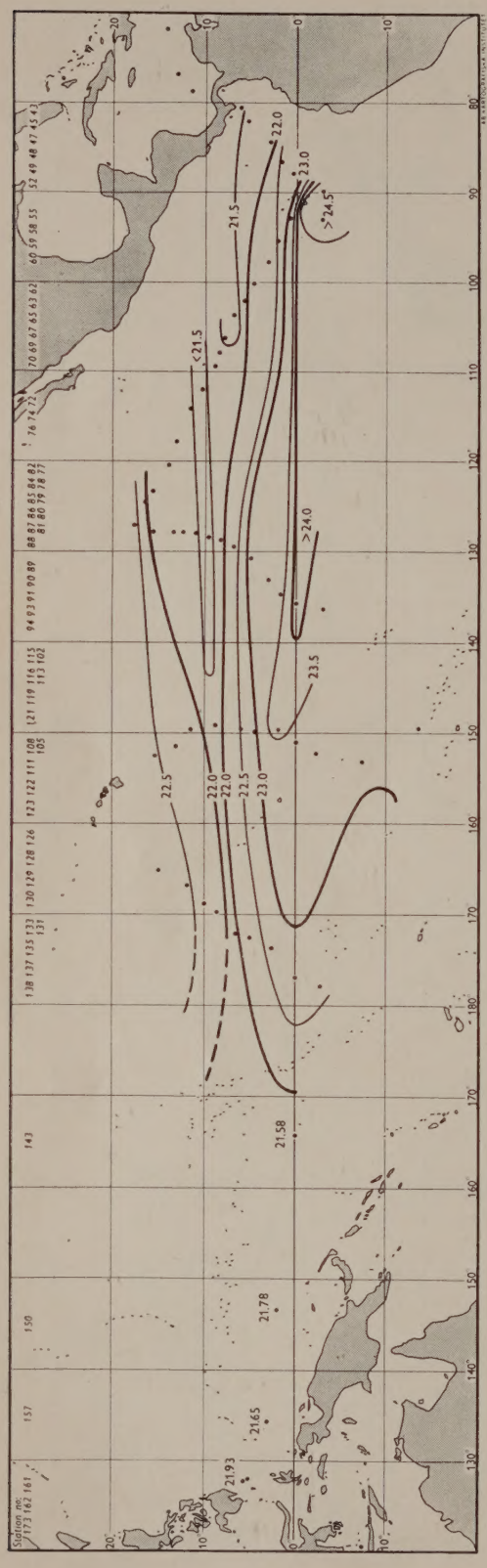

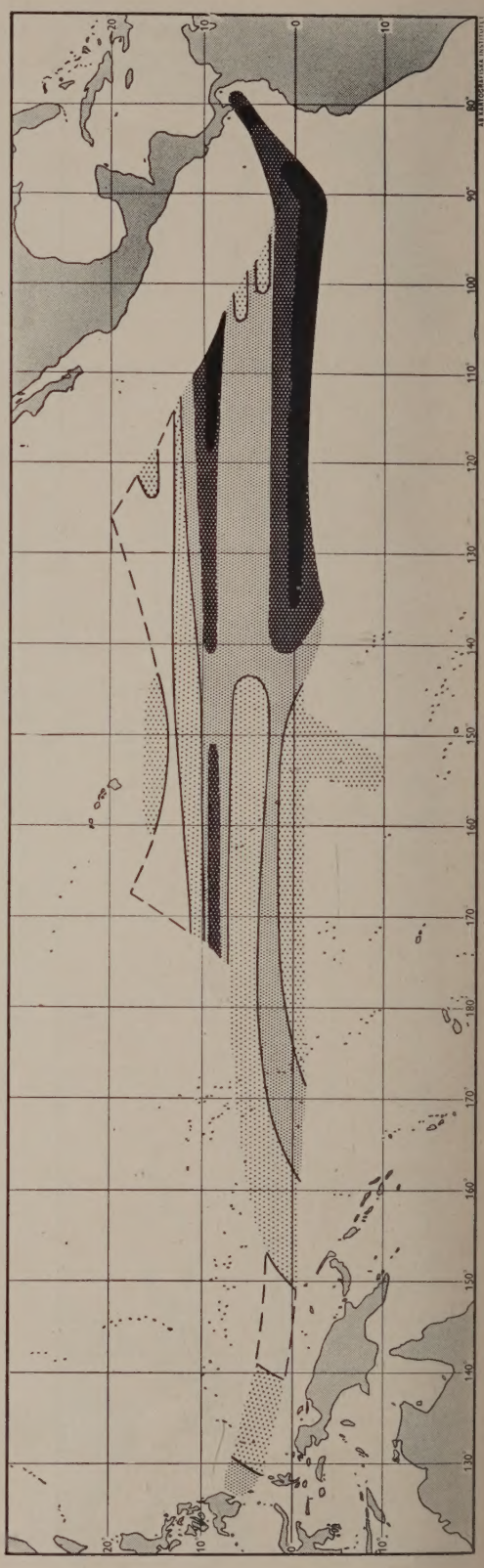

Fig. 6. Horizontal distribution of density (σ_t) at surface.

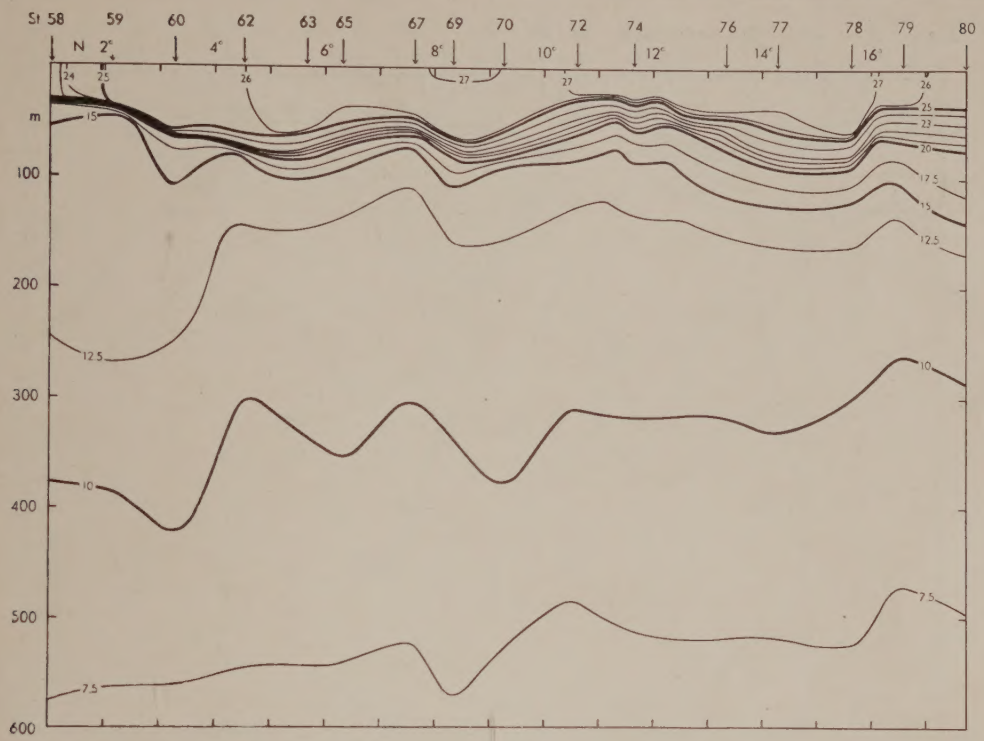

Fig. 8. Vertical distribution of temperature in Section 1.

particles was attained at Station 150 in the west Pacific.

We shall return to the particle distribution later when discussing the currents.

Vertical Distribution of Properties

The typical structure of the water masses in the equatorial current system appears in the vertical sections given in Figs. 8—23. Distributions for temperature, salinity, and density (σ_t) have been derived for all four sections. In addition oxygen, phosphate, silicate, and pH are represented in Section 3.

MONTGOMERY (1954) has suggested a new procedure for processing the observational data. He uses bathytermograms and T-S diagrams to arrive at a picture of the detailed variations of density between the serial stations. Then the density is selected as a reference variable in order to achieve consistency among different properties.

As we made bathythermograph lowerings to a nominal depth of 130 m only, details in the temperature distribution below this level are lacking. The general trend of the B. T. temperatures obtained (which are the least accurate data of all observations) between the serial stations has been considered, but minor variations chiefly due to internal waves and local wind effects have not been taken into account, being irrelevant in this connection. The plotting of isopleths for other properties have been guided by the σ_t-curves but with great caution considering their non-conservative character. It is not precluded that a spreading of these concentrations sometimes occurs along σ_t-surfaces. For instance, the 1.0 isopleth for phosphate almost coincides with the curve $\sigma_t = 25$ in Section 3 (Fig. 16 and 19).

We shall for a moment dwell upon the vertical distributions. Section 1 shows a rather complex structure due to two eddies which disturb the zonal flow. The density maximum

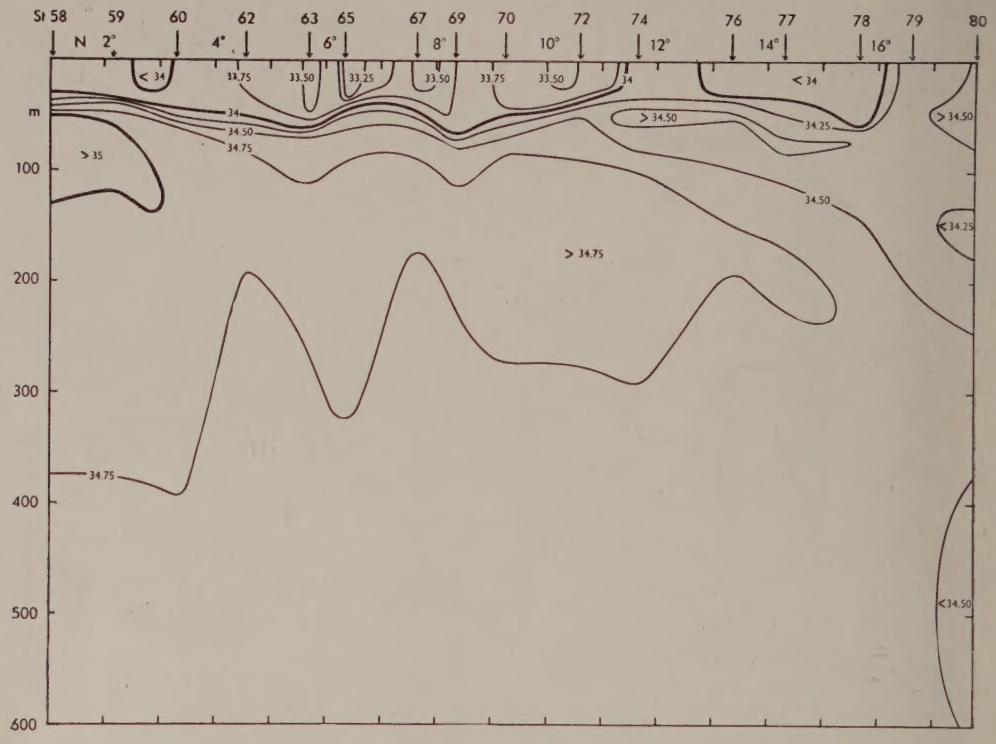

Fig. 9. Vertical distribution of salinity in Section 1.

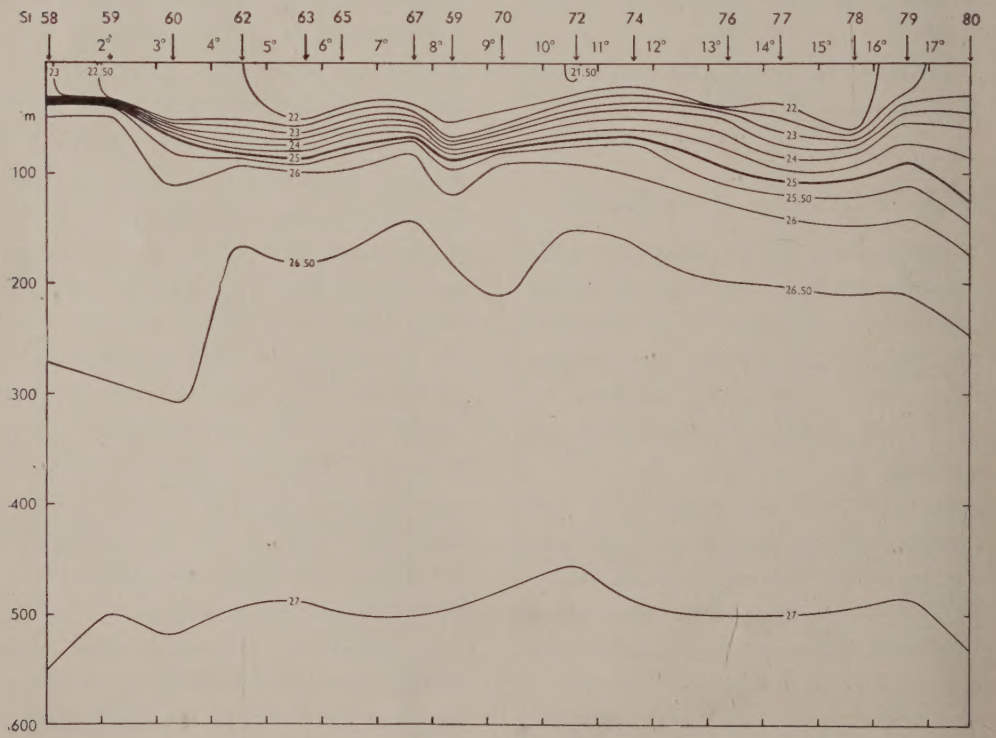

Fig. 10. Vertical distribution of density (σ_t) in Section 1.

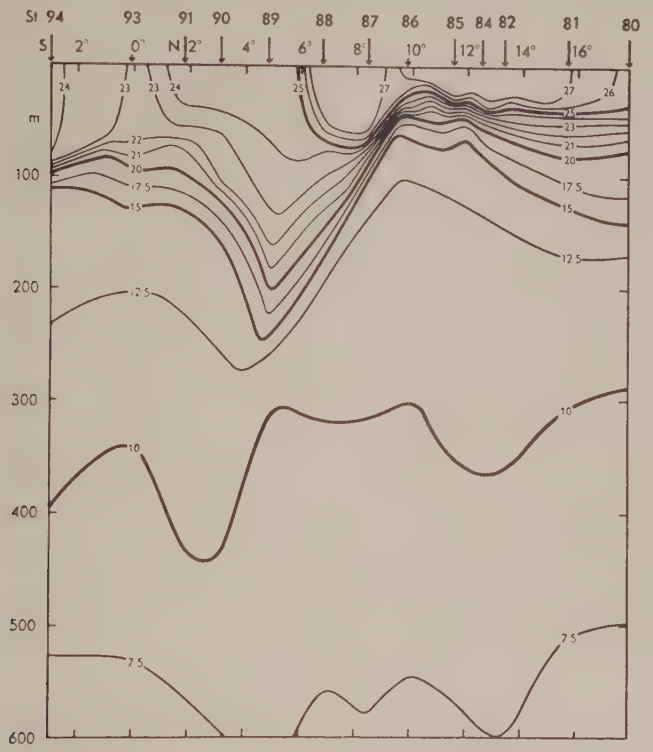

Fig. 11. Vertical distribution of temperature in Section 2.

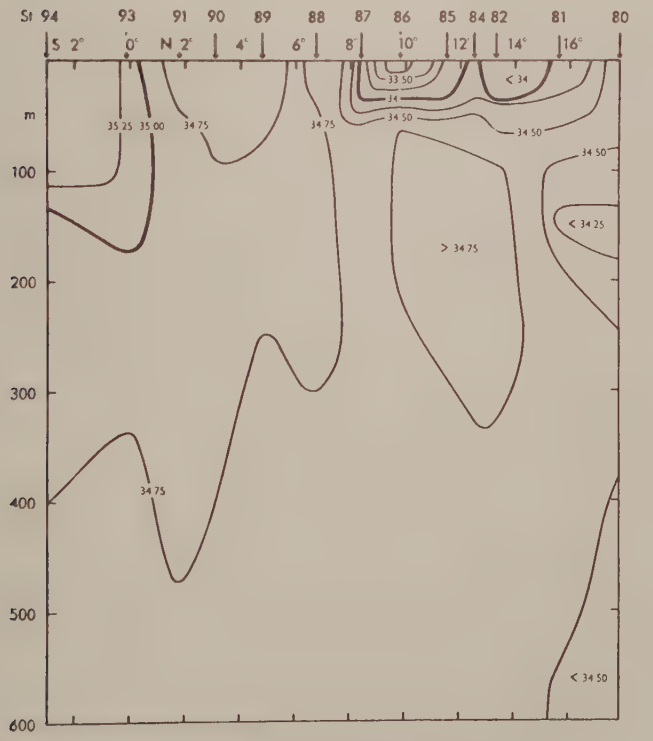

Fig. 12. Vertical distribution of salinity in Section 2.

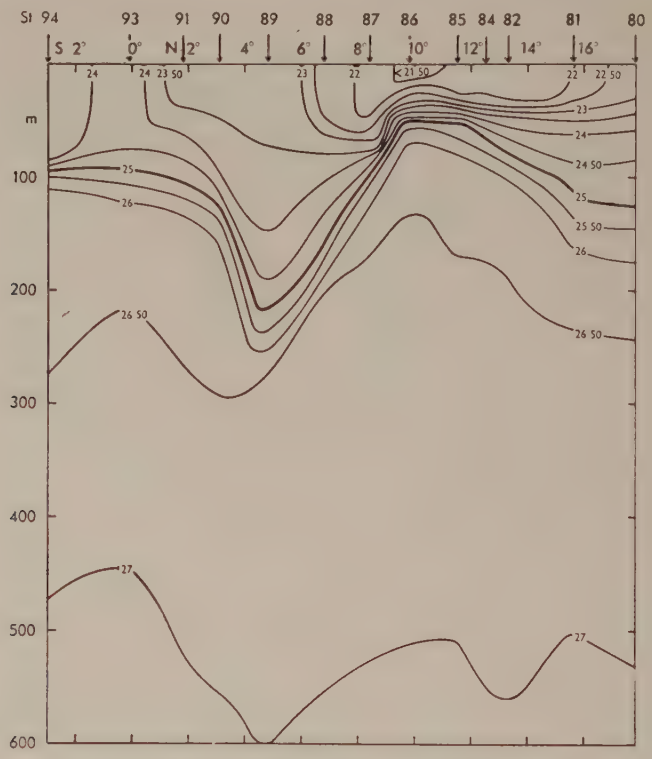

Fig. 13. Vertical distribution of density (σ_t) in Section 2.

near 11° N indicates the northern edge of the Countercurrent. The most conspicuous structure of the current system appears in Section 2. The minimum at 5° N indicates the southern edge of the Countercurrent whereas the salient rise of the isopleths and their close packing at 10° N reveals its northern edge.

The same characteristic features are found in Section 3, though somewhat less marked than in Section 2, in particular as to the deepening of the isopleths at the southern edge of the Countercurrent. The northern upheaval shows two separate maxima, one at 9°.5 N, the other at 13°.5 N.

The Countercurrent is displaced to the south in Section 4, with its minimum at 3° N. The northern maximum is rather flat but there is a sharp drop of the isopleths to the minimum.

In these diagrams there is clear evidence of upwelling at the Equator from the vertical orientation of the curves. Almost all isopleths for the different properties can be drawn without violation of the observed points so as to form a maximum or a minimum at or near the Equator, which is consistent with the dynamical conditions.

The discontinuity layer in the Pacific is best developed in the easter-most areas where it takes the character of a discontinuity surface (Fig. 10). Its thickness is also affected by the drop and the rise of the isopleths.

The discontinuity layer is, over large regions, associated with a salinity maximum (Defant, 1936, Sverdrup *et al.*, 1942) which originates from the subtropical convergences. This tongue of high-salinity water is clearly visible in Figs. 9 and 15. It is also well developed in the western regions, at stations 150, 157, and 162. Apparently such a maximum cannot be maintained as a continuous tongue in the current system where a marked vertical circulation occurs.

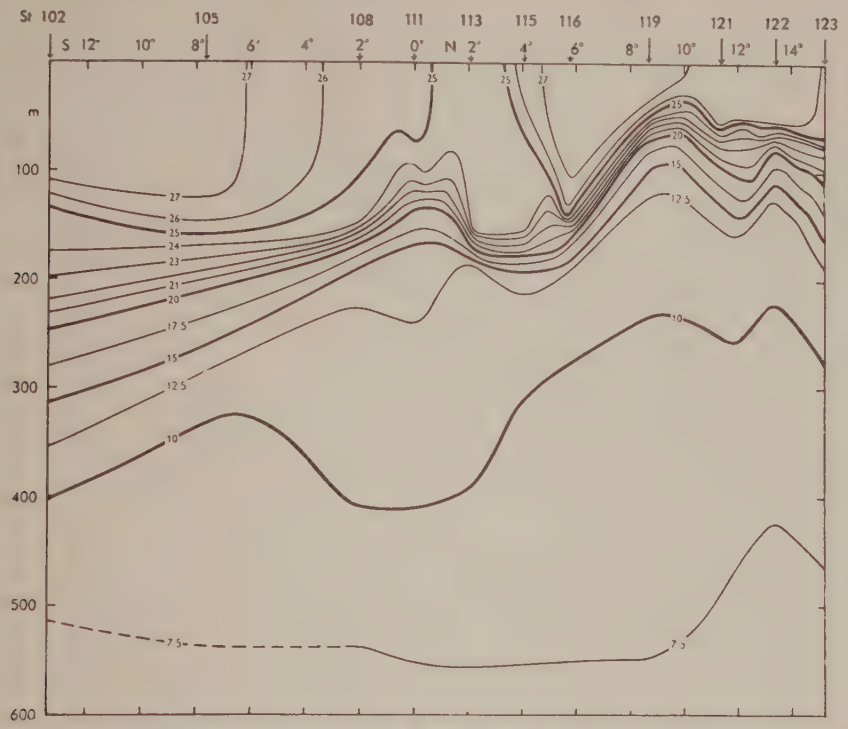

Fig. 14. Vertical distribution of temperature in Section 3.

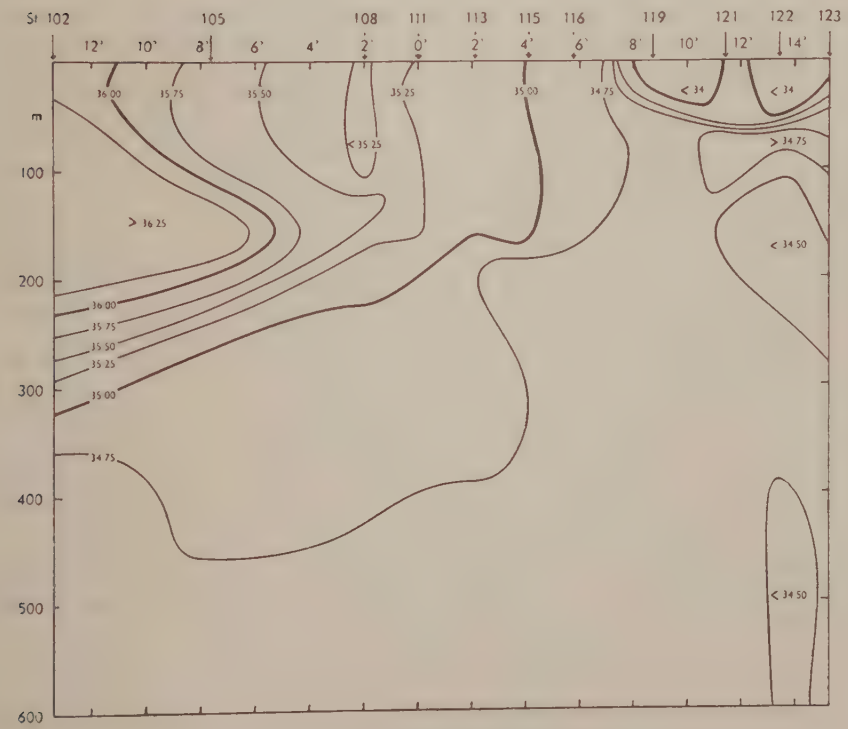

Fig. 15. Vertical distribution of salinity in Section 3.

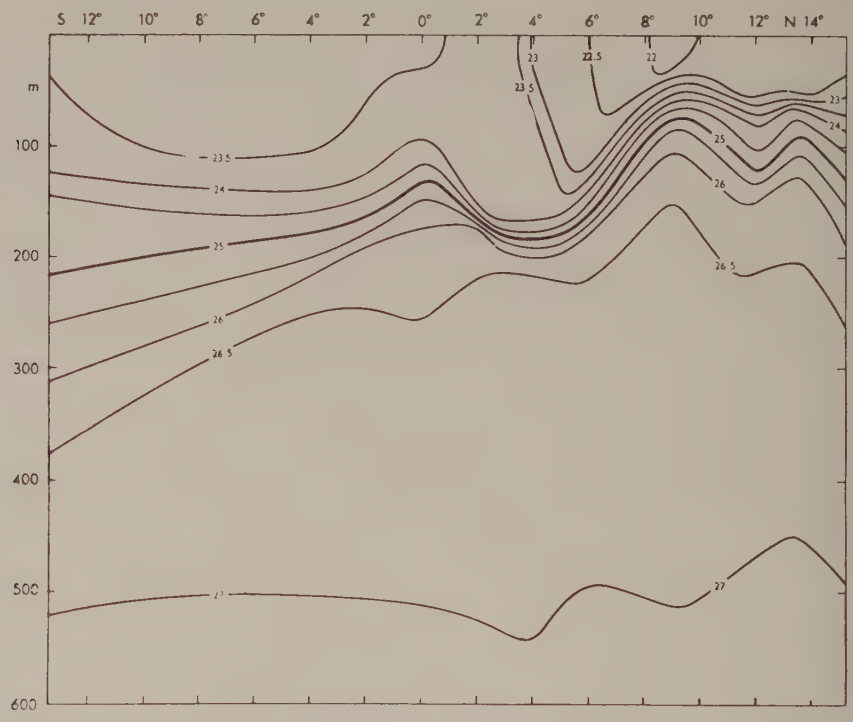

Fig. 16. Vertical distribution of density (σ_t) in Section 3.

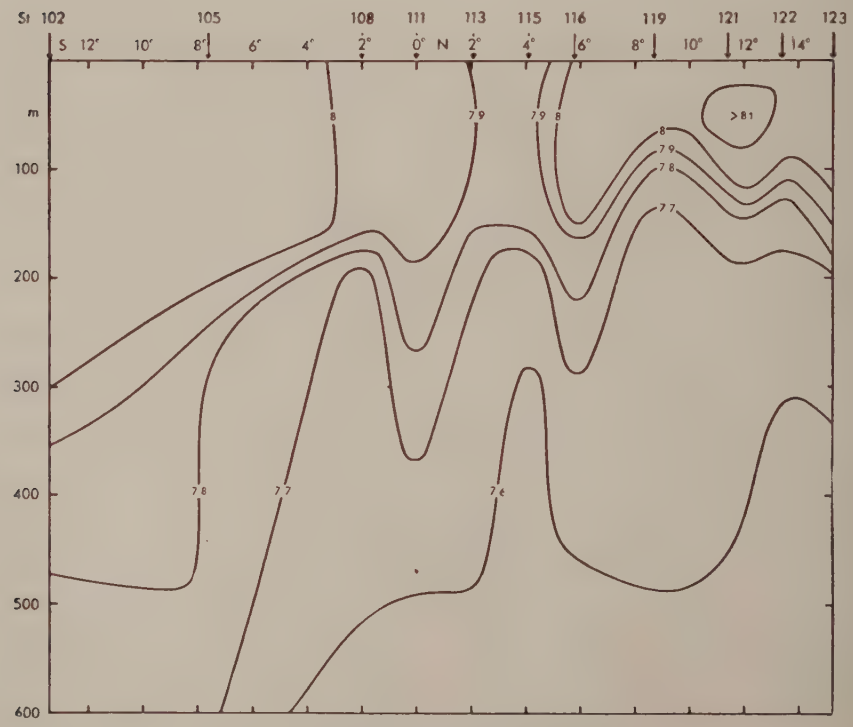

Fig. 17. Vertical distribution of pH in Section 3.

Fig. 18. Vertical distribution of oxygen in Section 3.

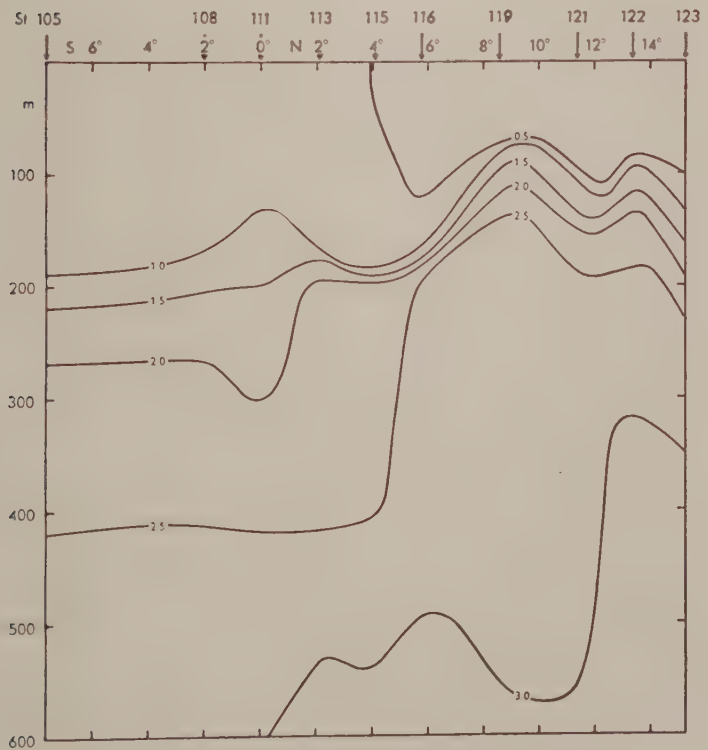

Fig. 19. Vertical distribution of phosphate in Section 3.

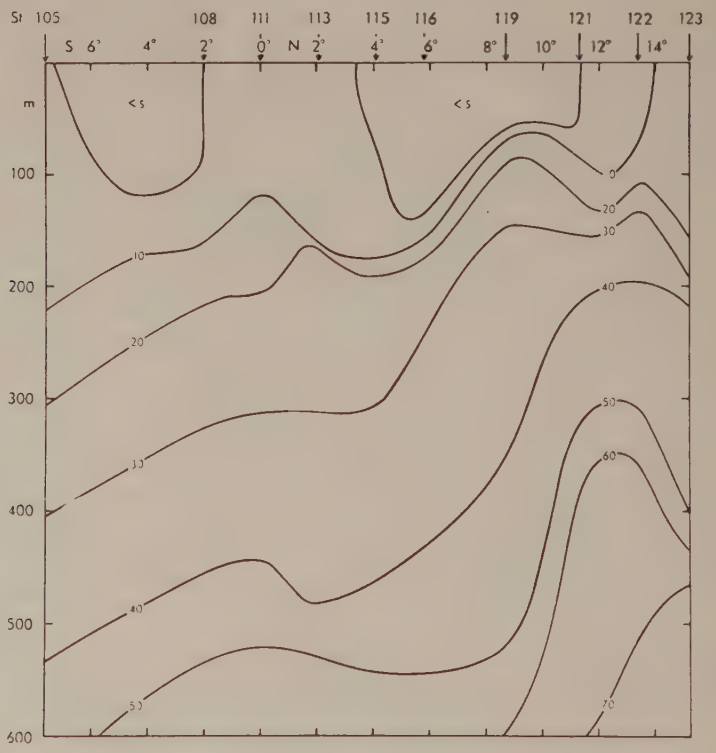

Fig. 20. Vertical distribution of silicate in Section 3.

It should also be mentioned that the tongue of low-salinity water (34.25—34.50 $^{0}/_{00}$), known from the *Carnegie* expedition, is present at 150—200 m in the northern parts of the sections (Figs. 9, 12, 15, and 22).

From the existing 4 sections of the density distribution it is possible to construct by interpolation three equidistant meridional cross-sections at long. 127°30′, 149°45′, and 172°00′ W respectively. Thus the experimental material is brought to a state suitable for the further interpretation of the currents (Figs. 24—26, Table 2).

TABLE 2. Oceanographic cross-sections

Cross-section	Time	Latitude	Longitude
I	Oct.	3° 00′ S—17° 46′ N	127° 30′ W
II	Nov.	7° 38′ S—15° 14′ N	149° 45′ W
III	Dec.	2° 37′ S—14° 39′ N	172° 00′ W

Absolute Topography of Isobaric Surfaces

DEFANT's (1941) procedure was employed in order to arrive at a representation of the absolute topography of the different isobaric surfaces on the basis of the computed anomalies of dynamic height. The depth of the reference layer, the layer of no motion, was found to lie between 500 and 900 m and nearest the sea surface at the Equator.

Derived values of dynamic heights for the sea surface are illustrated in Fig. 27, the Equator Station 111 being chosen as zero level. The sea surface south of the Galapagos Islands lies 30 cm below this level, whereas just north of the Equator at long. 180° it is 30 cm above the same. The steepness of the slope near the Equator, which is due to the westward wind stress and associated with a piling up of light surface water in the western Pacific, agrees well with previous estimates from

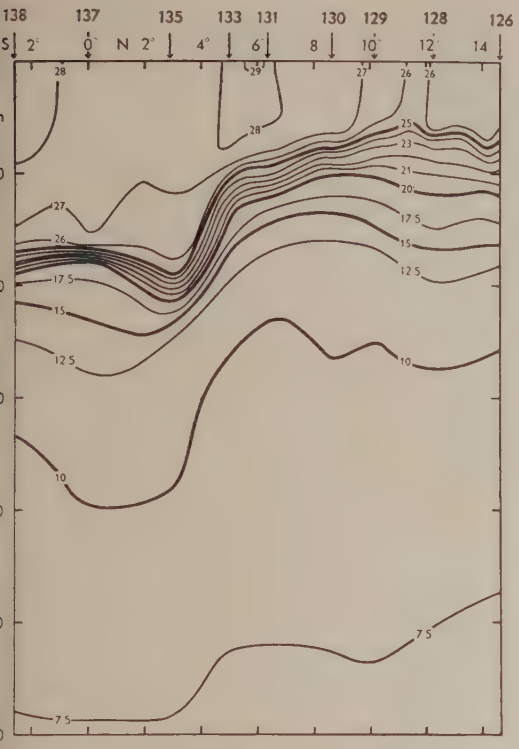

Fig. 21. Vertical distribution of temperature in Section 4.

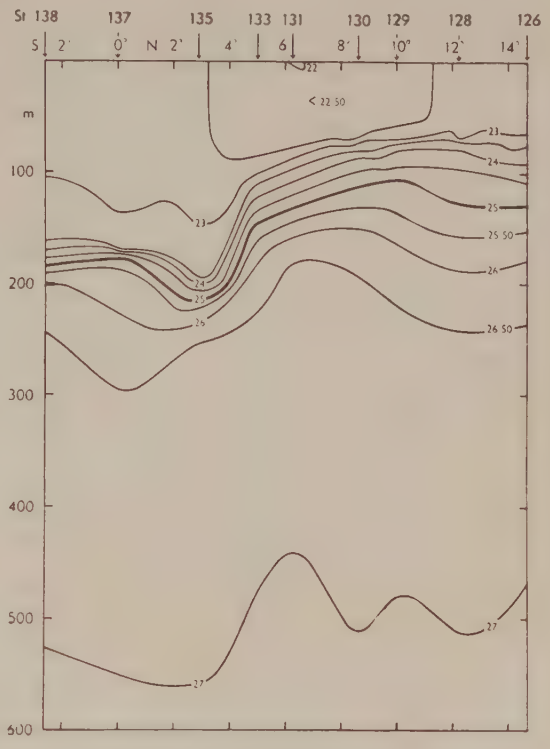

Fig. 23. Vertical distribution of density (σ_t) in Section 4.

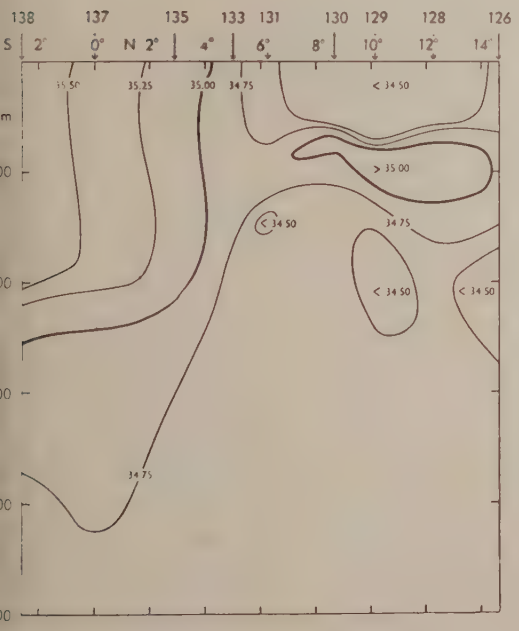

Fig. 22. Vertical distribution of salinity in Section 4.

the *Dana* results (MONTGOMERY and PALMÉN, 1940).

The prominent trough at the Equator gives evidence of the Equator Divergence and the ridge at 5° N, which towards the west gradually approaches the Equator, indicates the southern edge of the Countercurrent. In the West Pacific the extrapolation is somewhat uncertain. The figure also brings out in Section 1 two large eddies in the Countercurrent.

The other trough situated near 10° N, associated with the boundary between the Countercurrent and the North Equatorial Current is split up into two branches as shown for Sections 1 and 3. A similar tendency in Sections 2 and 4 is not distinguishable on the chart but it is manifest at lower isobaric surfaces.

It has been stated that the equatorial currents in the Pacific are closely related to the

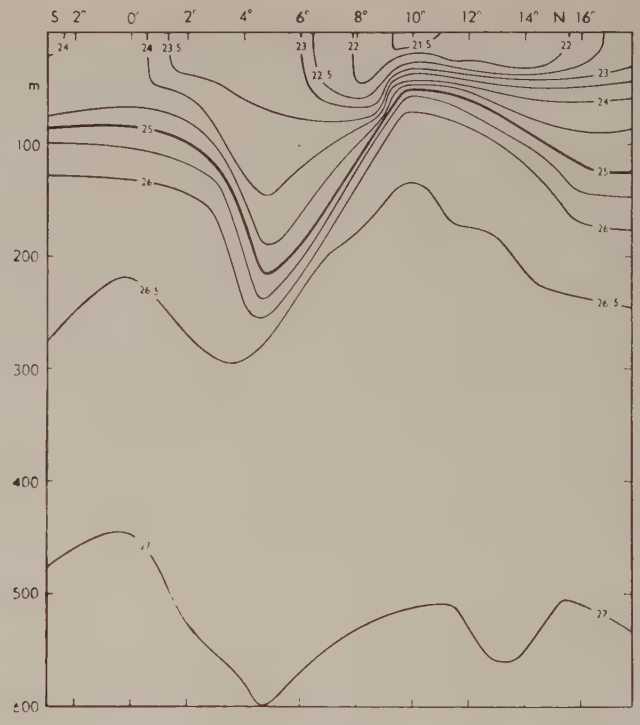

Fig. 24. Vertical distribution of density (σ_t) in Cross-section I (127° 30′ W).

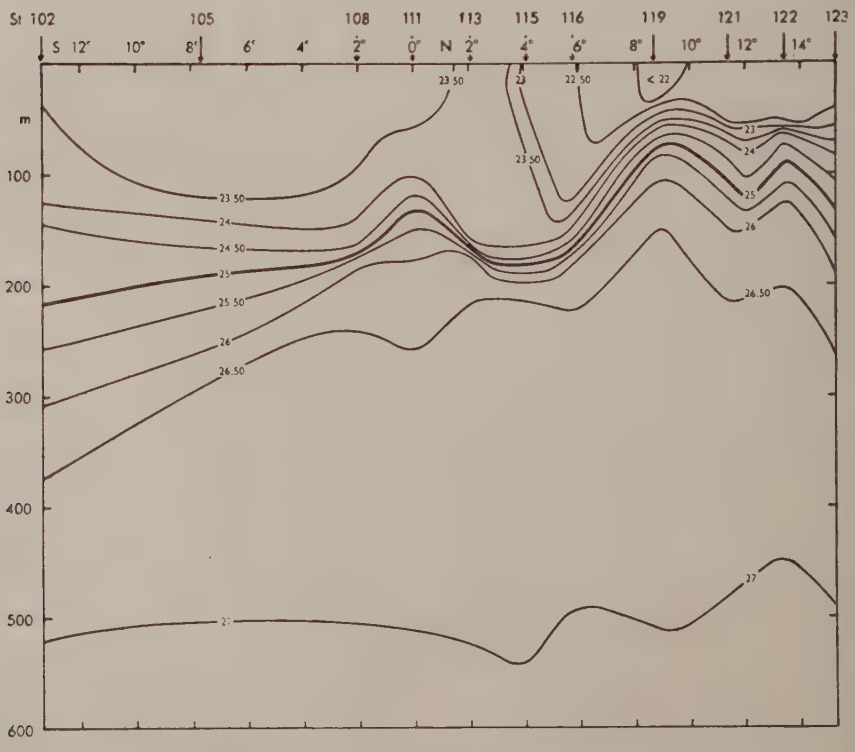

Fig. 25. Vertical distribution of density (σ_t) in Cross-section II (149° 45′ W).

slope of the discontinuity layer (SVERDRUP *et al.*, 1942). The density surface $\sigma_t = 24.5$ coincides with the maximum density gradient and roughly with the shallow salinity maximum in the Pacific. A representation showing the depth of this density surface (Fig. 28) is remarkably consistent with that in Fig. 27, troughs corresponding to ridges and *vice versa*.

In this connection attention is again drawn to the particle distribution (Fig. 7) which exhibits a striking resemblance to the dynamic topography. Even such details as the localized eddies are congruent. This may be understood from the fact that horizontal eddies bring a supply of nutrients from below (CROMWELL, 1951; MAO and YOSHIDA, 1953). It seems justified to consider the simple method of studying the particle distribution as a useful means of establishing regions of vertical movements in the sea.

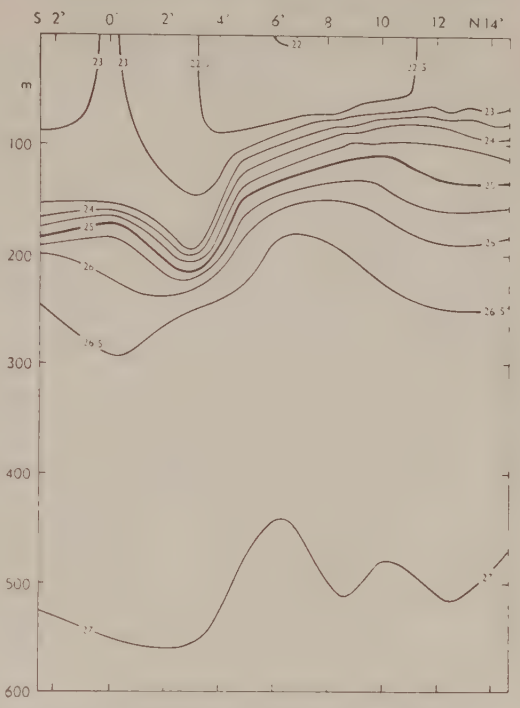

Fig. 26. Vertical distribution of density (σ_t) in Cross-section III (172° 00′ W).

Currents

The horizontal velocities in cm/sec. in the three cross sections have been geostrophically computed and are shown in Figs. 29—31. Near the Equator, where the Coriolis parameter is small, the computation is fictive. An attempt has been made to derive surface-current velocities from the drift of the vessel found from the ship's records with due regard to the wind drift. A comparison between these and the geostrophic values reveals, as anticipated, that the latter are much higher for the equatorial region. Because of the considerable wind drift of the *Albatross*, a 4 masted sailing ship, it does not seem justified to lay too much emphasis on this comparison. The velocity distribution is therefore not depicted at lower latitudes than 3°, which is the approximate limit for the validity of the classical formulae (WEENINK and GROEN, 1952). The boundary between westward and eastward flow is, however, illustrated also in the equatorial region.

Thus, the velocity distributions yield little information about the South Equatorial Current. Nevertheless it is clear that this current is actually present as a swift flow, attaining a maximum velocity of at least two knots in Cross-section I.

It is noticed that some features in the flow of the Countercurrent are common to all the cross sections. The Countercurrent is deeper and swifter towards its southern edge, the nucleus of its flow being centered at 75 m. It extends below the South Equatorial Current. CROMWELL, MONTGOMERY, and STROUP (1954) have directly observed this subsurface current by using deep drags.

Further it is noticed that the North Equatorial Current is interrupted by zones of easterly flow. This phenomenon appears in Cross-section I below 150 m only. The magnitude of such a weak current is of the same order as the errors inherent in the current determination, and its presence might be a fictive appearence due to the disturbing effect of internal waves.

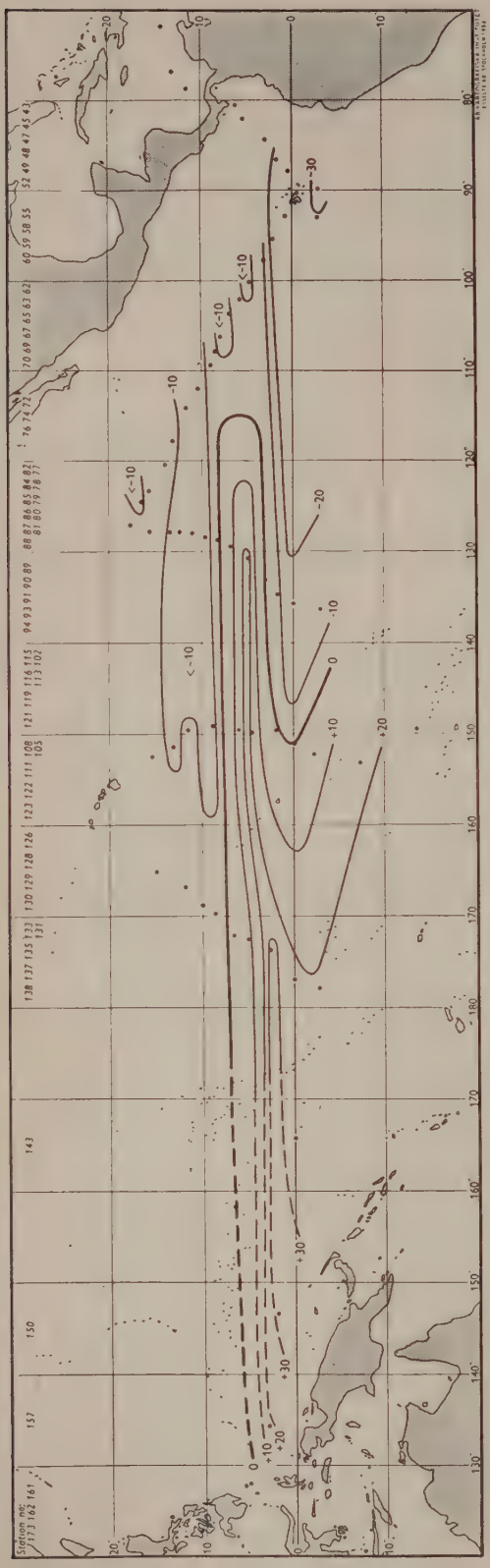

Fig. 27. Dynamic topography of the sea surface.

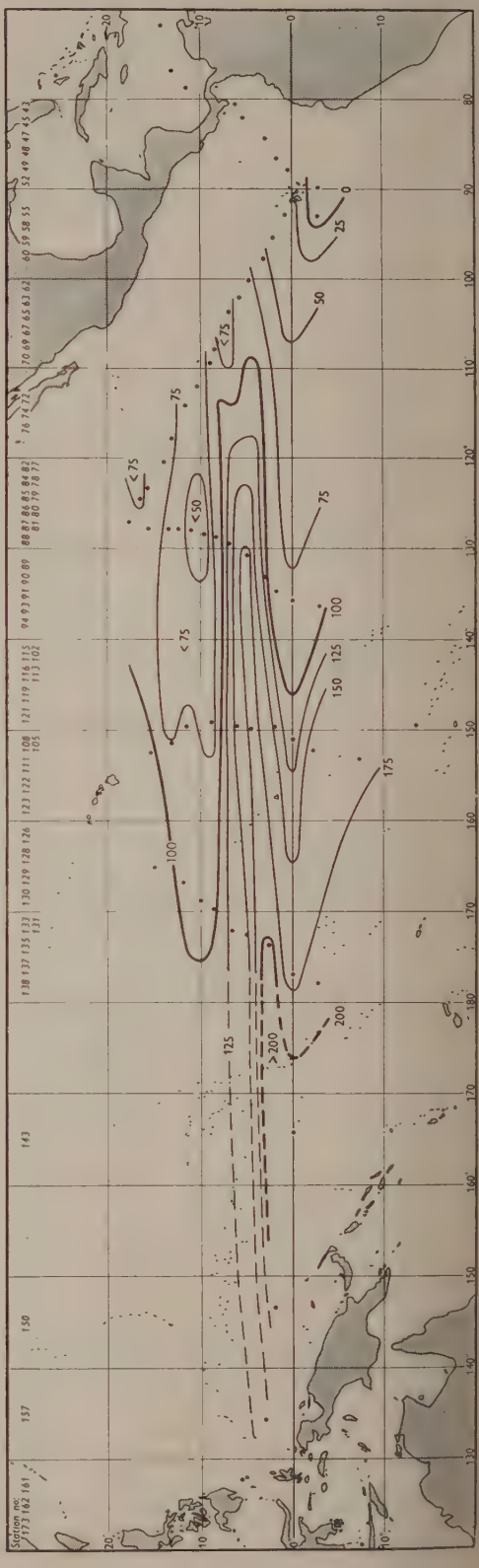

Fig. 28. Topography of the discontinuity layer ($\sigma_t = 24.5$).

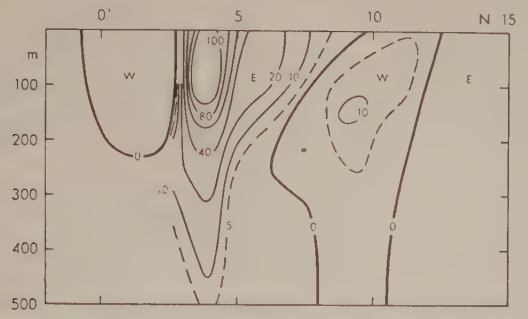

Fig. 29. Geostrophic currents (cm/sec.) in Cross-section I.

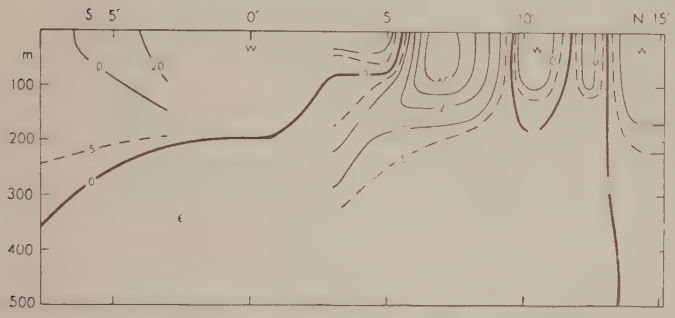

Fig. 30. Geostrophic currents (cm/sec.) in Cross-section II.

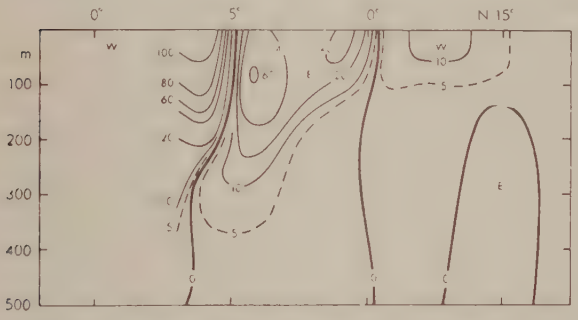

Fig. 31. Geostrophic currents (cm/sec.) in Cross-section III.

n Cross-section II, however, the current in question is stronger and penetrates the whole water column in conformity with the double maximum in Fig. 25. In this case the westward currents are fairly shallow and the whole body of deep water from 5° S to 12° N moves eastwards. Finally, the easterly current between 2° and 15° N in Cross-section III is too weak to admit of any definitive conclusions.

The geostrophic currents at the surface are represented as east-west vectors in Fig. 32 into which Section 1 is also incorporated. The main flow of the Countercurrent, which appears clearly, is indicated by curves. The position of its southern edge varies between 2.5° and 5° N, whereas the northern edge gradually moves southwards from 10° N in Section 1 to 9° in Section 4. The Countercurrent flows with a maximum velocity of 50—60 cm/sec. in the eastern areas. In the most westerly section a value of 100 cm/sec. or two knots is attained, which is due to the prevailing abnormal wind distribution which occasions a strong westward wind-stress over the northern parts of the

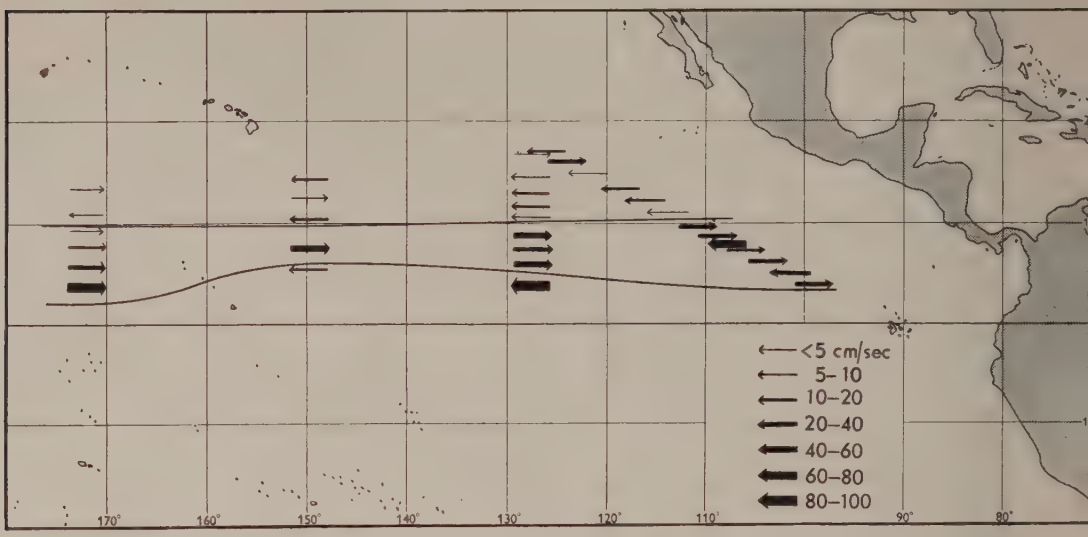

Fig. 32. Geostrophic currents at the surface represented as east-west vectors.

Countercurrent so that its main flow is largely concentrated towards the south, where the stress practically vanishes.

The problem of zonal flow may be looked upon from another angle, viz., the horizontal distribution of the total mass transport of water. This can be obtained by integration from the vertical distributions in Figs. 29—31. The use of the integrated equations of horizontal motion also takes the wind stress into account (SVERDRUP, 1947; REID, 1948). These differential equations have the form:

$$\frac{1}{\varrho}\frac{\partial}{\partial y}\left(A\,\frac{\partial M_x}{\partial y}\right)+ + \tau_x + 2\,\omega \sin\varphi\, M_y - \frac{\partial P}{\partial x} = 0 \qquad (1)$$

$$\frac{1}{\varrho}\frac{\partial}{\partial x}\left(A\,\frac{\partial M_y}{\partial x}\right)+ + \tau_y - 2\,\omega \sin\varphi\, M_x - \frac{\partial P}{\partial y} = 0 \qquad (2)$$

$$\frac{\partial M_x}{\partial x} + \frac{\partial M_y}{\partial y} = 0 \qquad (3)$$

where M_x and M_y are the components of mass transport, τ_x and τ_y those of wind stress (the x- and y-axis are taken positive eastwards ar northwards respectively, z is measured vert cally downwards).

The pressure integral P is defined as

$$P = \int_0^d p\,dz \qquad (4)$$

where p is the pressure and d the depth of r motion. It is sufficient to extend this int gration to 500 m only, as the contributio from deeper layers is negligible.

Applying equation (2) to the equatori current system we may consider the term lateral mixing as insignificant. Judging fro the conventional data on the average win stress in the Pacific (SIO, Oceanopraphic R port 14), the component τ_y is small compare with $\partial P/\partial y$. It may be mentioned that son facts argue in favour of the wind-stress bei underestimated at speeds less than 4 Beaufo (MUNK, 1950, WEENINK and GROEN, 1952 In any case the mass transport M_x is esse tially obtained from the density distributio and the computed values practically equ those derived by integration from Figs. 29—3

On the chart in Fig. 33 the computed valu of the mass transport M_x from surface

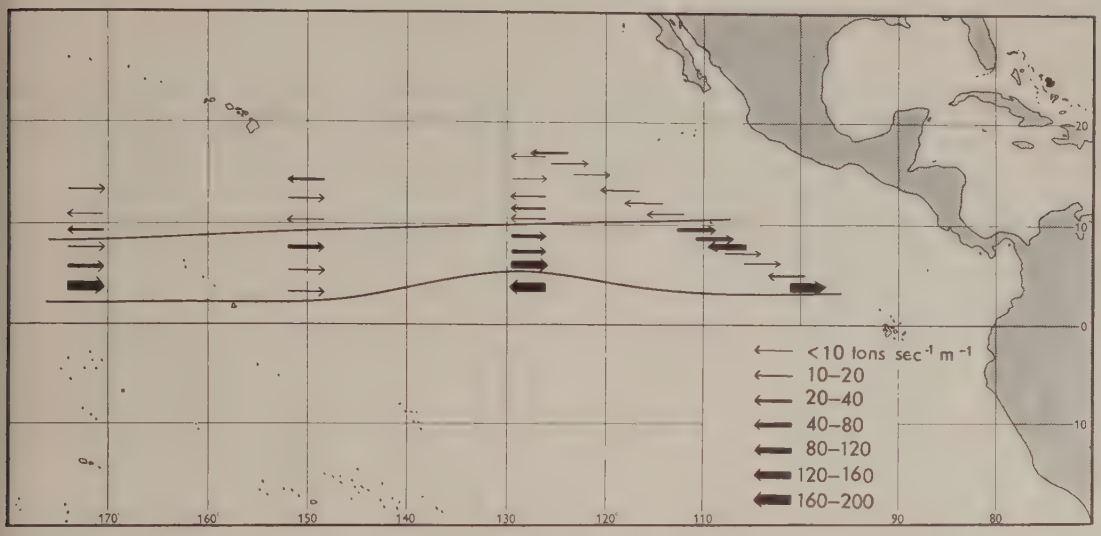

Fig. 33. Mass transport of water from surface to 500 m depth given as east-west vectors.

500 m are represented. It will be noticed that the transport is not everywhere congruent with the surface current. For instance, the transport vector is directed against the surface current in the southern part of the Countercurrent, at 150° W.

The total mass transport by the Countercurrent within the boundaries given in Fig. 33 was found to be

at 127° 30′ W ..... 36 million tons per sec.
149° 45′ 25
172° 00′ 43

These values are compared with that evaluated from *Carnegie* data which is representative for October and amounts to 25 million tons per sec. across the 140th meridian (Sverdrup *et al.*)

An interesting feature in the transport pattern is the region of eastlerly flow at 12°—15° N. One would be inclined to look upon this as an additional Countercurrent if the observations were not made at different times. In three of the sections the zone in question includes only one current determination, the existence of which as a flow of non-transient character is not established. On the other hand, the double density maximum in Cross-section II is apparently not illusory and such a phenomenon has also been observed by the American expeditions in several cases. As the Countercurrent is likely to meander at its northern limit because of the large velocity shear (Yoshida, Mao, and Horrer, 1953) the appearence of localized easterly flow may also be attributed to such large eddies, as have been encountered by the Shellback Expedition (Wooster, 1952).

It is beyond the scope of this report to enter into a detailed discussion of the theoretical aspect of the equatorial currents. Apart from the investigations quoted the theory has been advanced particularly by Stommel (1948), Hidaka (1949), Munk (1950), and Fofonoff (1954). It is evident from these interpretations that the mechanism of the equatorial currents may principally be understood from the action of the prevailing winds.

The equation system (1), (2), and (3) may be taken to represent the zonal and the meridional flow outside the region 3° S — 3° N. The terms of lateral mixing and of wind stress may be neglected in equation (2) but decidedly not in equation (1). A solution

accomplished for different integration regions indicates that the value of A, the kinematic eddy viscosity pertaining to lateral stresses, becomes less as the area considered grows. Thus, the A value is influenced by the dimensions of the current system studied. This is consistent with the finding of MUNK (1950) that the water transport in the oceanic circulation is almost independent of A.

Transverse Circulation

The vertical distributions so far discussed do not justify any decisive conclusion on the transverse circulation except as to the Equator Divergence. The presence of an upwelling extended to the surface at or near the Equator must be considered as an established fact, based on experimental as well as on theoretical evidence. On the other hand the vertical circulation towards the north contains some confusing features.

The theory of DEFANT (1936) based on the assumption of no net meridional transport ($M_y = 0$) requires a convergence at the southern boundary of the Countercurrent combined with pronounced sinking and a surface divergence at its northern boundary with upwelling.

CROMWELL (1953) reports that an Equatorial Front is sometimes encountered just north of the Equator. The front is associated with horizontal convergence and sinking but it does not coincide with the southern edge of the Countercurrent. A front of this kind was not observed onboard the *Albatross* in the Pacific, but instead near the Equator in the Atlantic.

CROMWELL and AUSTIN (1954) are not inclined to acknowledge the presence of an upwelling at the northern boundary of the Countercurrent but they do not preclude the possibility that a mixing caused by strong winds occasionally takes place in the upper stratum, which brings up nutrient-rich water. AUSTIN also discusses the definition of upwelling.

A theoretical model of the shallow water circulation in a vertical meridional plane has been advanced by YOSHIDA *et al.* This is characterized by a marked sinking at the southern boundary of the Countercurrent, and by a fairly strong upwelling at its northern boundary. The meridional water transport at the surface of the Countercurrent is directed towards the north.

It is worth while to consider for a moment the vertical distribution of particles across the equatorial currents. Conditions in Section 4 may be taken as an illustration (JERLOV 1953 a). It should be pointed out that Section 3 is rather similar to Section 4 in this respect whereas Sections 1 and 2 present a more complex structure, probably due to appreciable meridional currents at middepths. The distribution in Section 4 (Fig. 34) largely represents phytoplankton population and plankton remnants, as the supply of terrigenuous components in this area must be low. It is therefore apt to give a clear indication of the organic production and ultimately of the vertical water movements prevailing.

Near the Equator the high particle content at the surface together with the low content at middepths gives ample evidence of the Equator Divergence whereas sinking at 3° N at the southern edge of the Countercurrent is strongly suggested. Moreover, the abundance of particles in the surface stratum compared with their scarcity in the deeper strata in the region 8—10° N leads us involuntarily to assume that there is an ascending water movement along σ_t-surfaces which enriches the upper layers with nutrients. The maintenance of a surface particle distribution with a maximum at the northern edge of the Countercurrent, as illustrated in Fig. 7, would require that a supply of nutrients from below takes place not as a sporadic but as a fairly steady process.

As regards the transverse circulation within

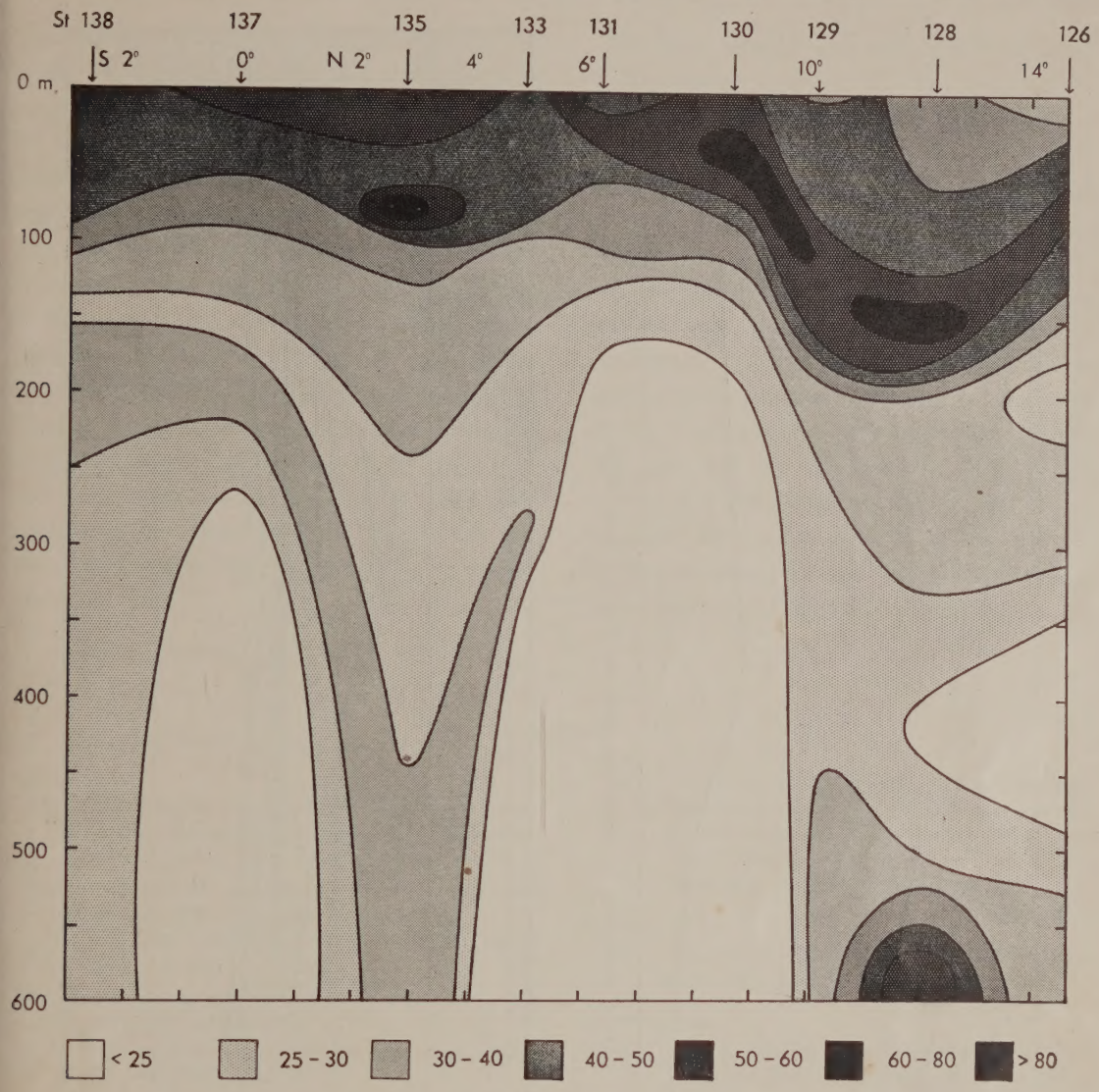

Fig. 34. Vertical distribution of particles in Section 4.

the Countercurrent, there are indications from the distribution of properties — besides the new theoretical evidence — that the water transport is towards the north at the surface. Another notable feature in Fig. 34 is that a maximum of particles appears as low as 150 at 12° N, where only a very restricted photosynthesis may take place. This is attributed to the wellknown effect of the discontinuity layer, so often demonstrated in transparency measurements. The accumulation of particles in the discontinuity layer is understood from the fact that the distribution of phytoplankton is chiefly governed by eddy diffusion which is greatly reduced within this layer.

Isentropic Analysis

Supplementary information about the general circulation is obtained by applying the isentropic analysis. A special interest is connected with the flow at the Equator where the deflecting force vanishes. Using *Dana* observations Montgomery and Palmén (1940) have shown

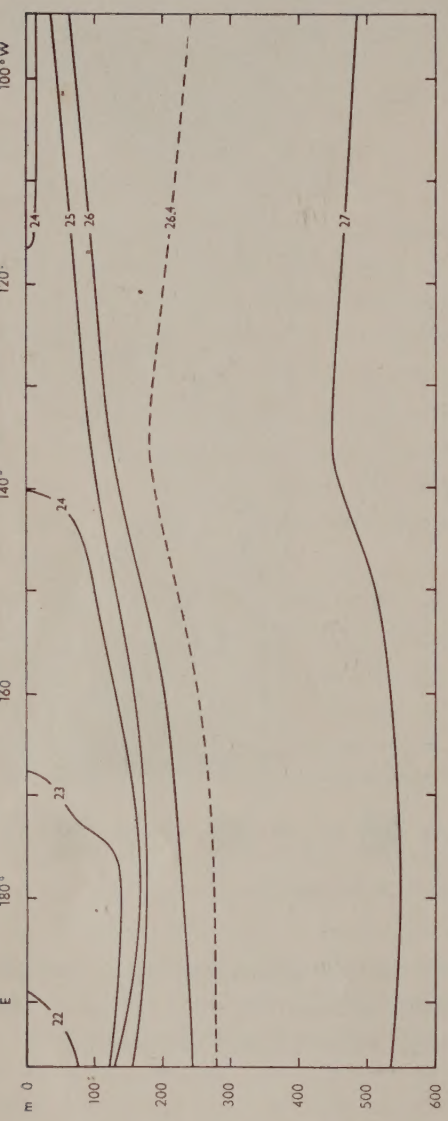

Fig. 35. Vertical distribution of density (σ_t) along the Equator in the Pacific.

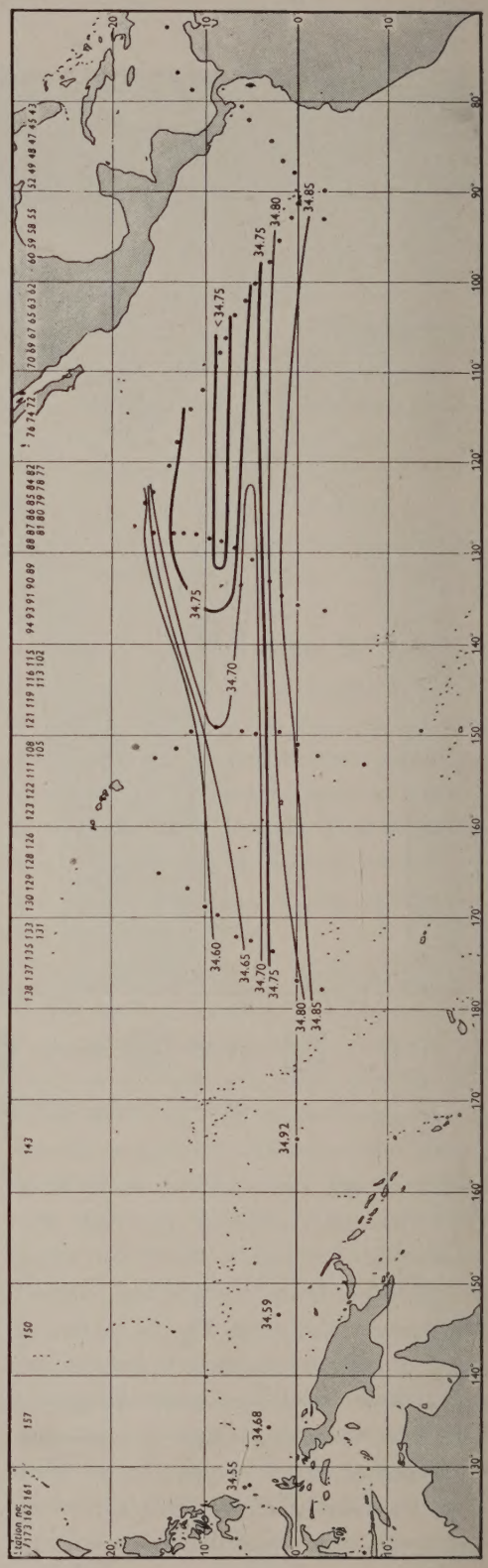

Fig. 36. Isohalines in the surface $\sigma_t = 26.6$.

that the wind stress exerted on the sea surface of the South Equatorial Current in the Pacific leads to a piling up of the light surface water in the western regions. The axial pressure gradient at the Equator, maintained by the trade wind, extends to about $\sigma_t = 26.4$ or to 200—250 m. The density distribution in Fig. 35 demonstrates this obliquity of the σ_t-lines in the upper strata whereas $\sigma_t = 26.4$ is almost parallel with lower isopleths. It appears to be a common feature for the South Equatorial Current in all three oceans that this surface is practically level (this volume, No. 5). The surface $\sigma_t = 26.4$ coincides roughly with the bottom of the discontinuity layer defined as the depth where the change in σ_t is 0.005 per m.

We have already seen that the topography of the surface $\sigma_t = 24.5$ in the discontinuity layer is closely related to the topography of isobaric surfaces (Fig. 28). Conditions well below the discontinuity layer may be represented by the salinity distribution in the surface $\sigma_t = 26.6$ which is between 200 and 400 m (Fig. 36). The trend of the isohalines indicate the presence of zonal flow. This is consistent with the fact that appreciable current velocities are found as far down as 400 m, the layer of no motion falling between 500 and 900 m. Though the large water transport occurs above the discontinuity layer we must also reckon with a motion below it sufficiently strong for distributing the isohalines according to the significant pattern.

References

Austin, T. S.

1954 a. Mid-Pacific oceanography III, transequatorial waters, August-October 1951. U. S. Fish and Wildlife Serv., Spec. Sci. Rep.: Fish. No. 131.

1954 b. Mid-Pacific oceanography V, transequatorial waters, May—June 1952, August 1952. U. S. Fish and Wildlife Serv., Spec. Sci. Rep.: Fish. No. 135.

Bruneau, L., N. G. Jerlov and F. Koczy.

1953. Physical and chemical methods. Reports of the Swedish Deep-Sea Expedition, v. 3, Physics and Chemistry No. 4.

Cromwell, T.

1951. Mid-Pacific oceanography, January—March 1950. U. S Fish and Wildlife Serv., Spec. Sci. Rep.: Fish. No. 54.

1953. Circulation in a meridional plane in the central equatorial Pacific. Jour. of Mar. Res., v. 12, No. 2, p. 196.

1954. Mid-Pacific oceanography II, transequatorial waters, June—August 1950, January—March 1951. U. S. Fish and Wildlife Serv., Spec. Sci. Rep.: No 131.

Cromwell, T., R. B. Montgomery and E. D. Stroup.

1954. Equatorial undercurrent in Pacific Ocean revealed by new methods. Science, v. 119, No. 3097, p. 648.

Defant, A.

1936. Die Troposphäre. Deutsche Atlantische Exped. Meteor, 1925—1927, Wiss. Erg., Bd. VI, Teil 1, 3. Leif., p. 289.

1941. Die absolute Topographie des physikalischen Meeresniveaus und der Druckflächen, sowie die Wasserbewegungen im Atlantischen Ozean. Deutsche Atlantische Exped. Meteor 1927—1927, Wiss. Erg., Bd. VI, 2 Teil. 5 Lief., p. 191.

Fofonoff, N. P.

1954. Steady flow in a friction-less homogenous ocean. Jour. Mar. Res., v. 13, p. 254.

Hidaka, Koji.

1951. Drift currents in an enclosed ocean. Part III. Geophys. Notes: Geophys. Inst., Tokyo Univ., v. 4, No. 3.

Jerlov, N. G.

1953 a. Particle distribution in the ocean. Rep. Swedish Deep-Sea Exp., v. 3, No. 3.

1953 b. Studies of the equatorial currents in the Pacific. Tellus, v. 5, No. 3, p. 308.

Mao, Han-Lee and Kozo Yoshida.

1953. Physical oceanography in the Marshall Islands area, Univ. of Calif., Scripps Inst. of Oceanogr. Ref. 53—27, April 15, 1953.

Montgomery, R. B.

1954. Analysis of a Hugh M. Smith oceanographic section from Honolulu southward across the Equator. Jour. of Mar. Res., v. 13, No. 1, p. 67.

Montgomery, R. B., and E. Palmén.

1940. Contribution to the question of the Equatorial Counter Current, Jour. Mar. Res., v. 3, p. 112.

MUNK, W. H.
1947. A critical wind speed for air-sea boundary processes. Jour. Mar. Res., v. 6, p. 203.
1950. On the wind-driven oceanic circulation. J. Meteorol., v. 7, p. 79.

REID, R. O.
1948 a. The equatorial currents of the eastern Pacific as maintained by the stress of the wind. Journ. Mar. Res. v. 7, p. 74.
1948 b. A model of the vertical structure of mass in equatorial wind-driven currents of a baroclinic ocean. Jour. Mar. Res., v. 7, p. 304.

ROSSBY, C.-G.
1936. Dynamics of steady ocean currents in the light of experimental fluid mechanics. Pap. phys. Oceanogr. Meteorol., v. 5, No 1.

SCHOTT, G.
1935. Geographie des Indischen und Stillen Ozeans. Hamburg. Verlag von C. Boysen.
1943. Weltkarte. Ann. d. Hydrogr. u. Mar. Meteorol. Tafel 22.

STOMMEL, H.
1948. The westward intensification of wind-driven ocean currents. Trans. Amer. geophys. Un., v. 29, p. 202.

STROUP, E. D.
1954. Mid-Pacific oceanography IV, transequatorial waters, January—March 1952. U. S. Fish and Wildlife Serv., Spec. Sci. Rep.: Fish. No. 135.

SVERDRUP, H. U.
1947. Wind-driven currents in a baroclinic ocean; with application to the equatorial currents of the eastern Pacific. Proc.nat. Acad. Sci., v. 33, p. 318.

SVERDRUP, H. U. and J. FLEMING.
1944. Scientific results of cruise VII of the CARNEGIE, 1928—29. Oceanography I—A: Observations and results in physical oceanography. II: Results in physical oceanography. Publ. Carnegie Inst., v. 545, p. 83.

SVERDRUP, H. U., M. W. JOHNSON and R. H. FLEMING.
1942. The oceans, their physics, chemistry, and general biology. New York: Prentice-Hall, Inc.

WEENINK, M. P. H. and PIER GROEN.
1952. On the computation of oceanic surface current velocities in the equatorial region from wind data. Koninkl. Nederl. Akad. Weten., Proc., (B) v. 55, p. 239.

WOOSTER, W. S.
1952. Preliminary report, Shellback Expedition, 17 May to 28 August 1952. SIO Reference 52—47 (unpublished).

WOOSTER, W. S. and F. JENNINGS.
1955. Exploratory oceanographic observations in the eastern tropical Pacific, January—March, 1953. Californian Fish and Game, v. 41, p. 79.

YOSHIDA, KOZO, HAN-LEE MAO and P. L. HORRER.
1953. Circulation in the upper mixed layer of the equatorial north Pacific. Jour. Mar. Res., v. 12, p. 99.